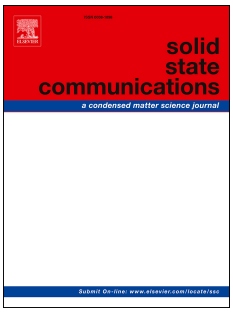

Influence of charge carriers on corrugation of suspended graphene

Demid A. Kirilenko, Andrei Gorodetsky, Marina V. Baidakova

PII: S0038-1098(17)30358-7

DOI: 10.1016/j.ssc.2017.11.003

Reference: SSC 13316

To appear in: *Solid State Communications*

Received Date: 13 July 2017

Revised Date: 24 October 2017

Accepted Date: 7 November 2017

Please cite this article as: D.A. Kirilenko, A. Gorodetsky, M.V. Baidakova, Influence of charge carriers on corrugation of suspended graphene, *Solid State Communications* (2017), doi: 10.1016/j.ssc.2017.11.003.

Influence of charge carriers on corrugation of suspended graphene

Demid A. Kirilenko[a,b], Andrei Gorodetsky[c,d], Marina V. Baidakova[a,b]

[a] *Ioffe Institute, Politekhnicheskaya ul. 26, 194021 St-Petersburg, Russia*
[b] *ITMO University, Kronverksky pr. 49, 197101 St. Petersburg, Russia*
[c] *Lancaster University, Lancaster LA1 4YW, UK*
[d] *Cockcroft Institute of Accelerator Science, Warrington WA4 4AD, UK*

Abstract

Electronic degrees of freedom are predicted to play a significant role in mechanics of two-dimensional crystalline membranes. Here we show that appearance of charge carriers may cause a considerable impact on suspended graphene corrugation, thus leading to additional mechanism resulting in charge carriers mobility variation with their density. This finding may account for some details of suspended graphene conductivity dependence on its doping level and suggests that proper modeling of suspended graphene-based device properties must include the influence of charge carriers on its surface corrugation.

Keywords:

The unique electronic properties of graphene are the core feature of this two-dimensional material. Charge carriers dynamics became the main subject of the related research since the very confirmation of graphene's most intriguing property – quasi-relativistic dispersion relation [1]. Moreover, the research in the field has been considerably encouraged by the high electron mobility in graphene that makes it quite perspective material for high-speed electronics. The investigation of free-standing (suspended) graphene is of special interest since the record values of electron mobility[2, 3, 4, 5] have been demonstrated for this very case. At the same time, the physics of the electron transport in

Email address: demid.kirilenko@mail.ioffe.ru (Demid A. Kirilenko)

suspended graphene becomes more complicated because of graphene extension into the third dimension. Electrons are scattered by the sheet undulations [6, 7] and for the case of pristine graphene it is suggested that its transport properties are governed by the interaction with flexural phonons (out-of-plane oscillations) [8, 9, 10, 11]. For instance, this leads to a limit for suspended graphene conductivity that is unavoidably present at non-zero temperature.

The flexural phonons are considered to be the main cause [12] of the pronounced corrugation of suspended graphene which was first detected by transmission electron microscopy (TEM) [13, 14]. Besides that, interaction between charge carriers and lattice undulations may significantly affect the corrugation of graphene [15, 16] and even may lead to a specifically corrugated state as it has been suggested in several works [17, 18, 19, 20, 21]. These results suggest that graphene can be considered as an "electronic membrane" where electronic and mechanical degrees of freedom are strongly coupled and proper portraying of its electronic properties should require consideration of its surface corrugation characteristics . For example, calculation of Volt-Ampere Characteristic (VAC) for an ordinary suspended graphene-based field-emission transistor must account for the flexural phonons suppression by the back gate induced strain [22].

An important consequence from this is that the investigation of the charge carriers effect on the corrugation can not be performed using electrostatic doping of graphene; because in this case the external electrostatic force unavoidably acting on the sheet significantly disturbs the corrugation dynamics. For this reason, we had to use another way for charge carriers generation in suspended graphene, and we exploited electron-hole pairs generation under the electron beam of TEM, that leaves the rest of the intrinsic graphene physics rather untouched. At the same time, in situ observed electron diffraction patterns allow to track variations of the suspended graphene corrugation [23, 24, 25, 26, 27, 28].

Here, we present the experimental results revealing the influence of generated charge carriers on the corrugation of suspended graphene. The results allow for the evaluation of the corresponding impact on the flexural phonons dynamics and the transport properties of graphene.

Graphene flakes were deposited on a conventional lacey carbon film on a TEM copper grip. A lacey carbon film has holes $1-5\ \mu m$ in diameter, thus, providing the corresponding sizes of graphene free-standing areas. We used graphene obtained by a chemical route [29] which is characterized by well-preserved crystalline structure, that makes it possible to utilize electron diffraction analysis, and relatively low content of ad-species on graphene surface. At the same time, we do find it essential to perform the experiments on partially oxidized graphene because the appearance of a bandgap Eg ca. 1 eV [30, 31, 32] considerably increases carriers lifetime up to $\tau \approx 10^{-8}s$ [33, 34] and, thus, the carrier density generated by the electron beam can reach practically relevant values. The use of partially oxidized graphene is crucial since the carrier lifetimes in pristine graphene are of the order of $10^{-13}s$ [35, 36] which prevents achieving reasonable carrier densities in our case. Whereas, ad-species does not affect considerably the flexural phonons dynamics and corresponding mechanical properties of graphene up to the surface coverage of ≈ 0.9 [37].

The charge carrier concentration in this experimental set-up can be varied by the intensity of the illuminating beam (Figure 1). The generated electron-hole pairs density can be evaluated using Bethe formalism with the modification of the incident electron energy loss derivative to the total average energy loss after graphene penetration and corresponding substitution of the total electron volume concentration used in Bethe formula by the surface density. The average quantity of electron-hole pairs created by an incident electron, then, can be multiplied by the electron beam current density and carrier lifetime in order to get the generated carrier density n_g:

$$n_g = \frac{2\pi n}{EE_g}\left(e^2 k_e\right)^2 \ln\frac{4E}{I} \times \frac{J}{eS} \times \tau. \tag{1}$$

Here, n is the total electron density in graphene, which is $2.2 \times 10^{16}\ m^{-2}$, E is the incident electron energy, E_g is the material bandgap, e is the electron charge, k_e is the electrostatic constant, I is the mean excitation potential, which is $78\ eV$ for carbon atoms [38], J is the electron beam current, S is the area of the

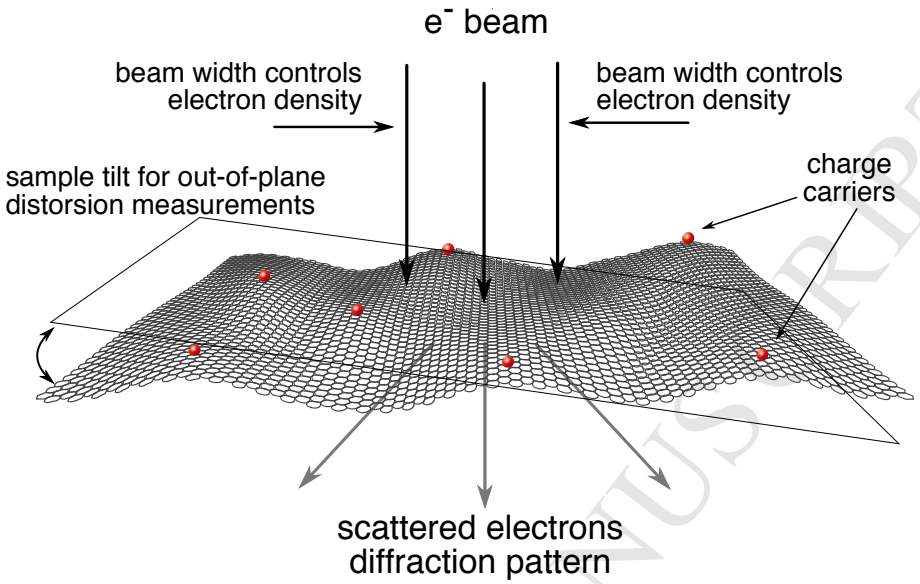

Figure 1: Schematic of the experiment. The electron beam of TEM generates charge carriers, so that their density varies when the beam current density changes. The scattered fast electrons form a diffraction pattern, which than acquired at a set of crystal tilts to get the information on the out-of-plane distortions of the crystal structure.

electron beam spot. For the given values of $E = 200\ keV$, $J = 1.2\ nA$ (the experiments were performed using transmission electron microscope JEM-2100F, Jeol, Japan), we estimate that at the beam size of 1 μm the generated charge carriers density should be $n_g \approx 10^{12}\ cm^{-2}$. We also performed measurements of less influenced graphene by spreading the beam up to 3 μm, thus lowering the charge carriers density by an order of magnitude to $n_g \approx 10^{11}\ cm^{-2}$. Measurement at lower beam current densities is hampered by the corresponding decrease of the intensity in the electron diffraction images and, thus, noticeable decrease of the signal-to-noise ratio. Whereas, measurement at higher beam current densities is limited by the radiation damage threshold of graphene. At the same time, we have to perform the experiments at 200 keV beam energy because it provides better beam spatial coherency, than at lower voltages, which is crucial for the resolution of the used technique and, thus, for the corrugation

analysis at the long-wavelength part of the spectrum.

It is worth noting, that at the given incident electron beam current densities the degree of irradiation defects emerging during the time of one experiment (ca. 5 min) stays well below 10^{-3} according to [39] and, thus, does not considerably affect the overall measurements. Similarly, the heating of the crystal, that is the result of energy transfer from the incident electrons to the phonons, remains negligible mainly due to the high thermal conductivity of the suspended graphene [40, 41, 42], which is defined by flexural phonons dynamics at ambient temperatures [43, 44, 45], and does not exceed several Kelvins in our case. It is also important that the sheet strain induced by the heating is limited by relatively low levels ca. $10^{-6} - 10^{-5}$ [46, 47, 48, 49]. In this case, the corrugation may only be affected at rather small wavevectors below $0.01 - 0.1\ nm^{-1}$ [50, 51] which are even inaccessible for the used measurement technique.

The corrugation of the suspended graphene is measured by the technique based on the analysis of electron diffraction patterns variation with the crystal tilt against the incident electron beam [52]. The technique allows measuring the Fourier components $H(q)$ of the crystal relief autocorrelation function $H(r)$; and, if we consider the corrugation as a manifestation of the flexural phonons, directly provides the flexural phonons spectrum. However, since some sort of uncertainty might be admitted concerning the complex mechanism of the corrugation formation we will further refer to the measured $H(q)$ as to the corrugation spectrum, which can be considered as a sum of possible static corrugation and dynamic corrugation caused by flexural phonons. The diffraction patterns were acquired from the graphene sheet area 100 nm in size using corresponding selective aperture in TEM.

Figure 2 presents the measured profiles of the suspended graphene corrugation in log-log scale for the two charge carriers densities. The plot for the lower density has much higher noise due to the lower electron beam intensity used in this case.

The most remarkable result here is the decrease of the corrugation spectrum at its long-wavelength part when the charge carrier density increases. The corru-

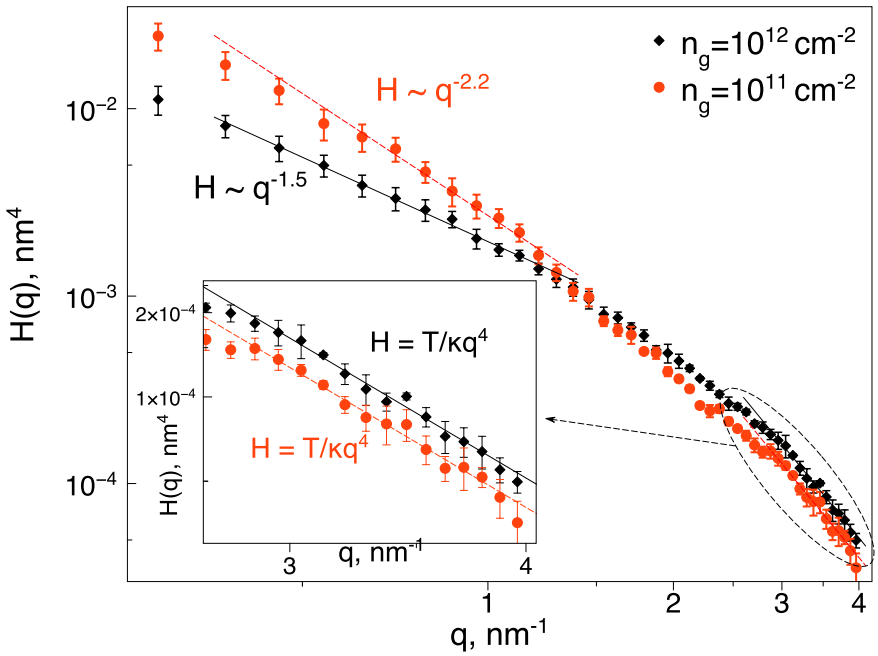

Figure 2: Corrugation spectrum profile measured at different charge carriers densities $n_g \approx 10^{11}\ cm^{-2}$ (red) and $n_g \approx 10^{12}\ cm^{-2}$ (black). Spectrum exponents at the long-wavelength part are marked to show the exponent decrease with increasing charge carriers density. Inset shows fittings of the spectrum profile at the short-wavelength part, where it follows the $\sim q^{-4}$ law coming from the harmonic approximation and is defined by temperature T and bending rigidity κ of the suspended graphene only.

gation amplitude correspondingly decreases from 3.2 Å at $n_g \approx 10^{11}\ cm^{-2}$ down to 1.7 Å at $n_g \approx 10^{12}\ cm^{-2}$. Moreover, the exponent of the spectrum profile significantly decreases from -2.2 at $n_g \approx 10^{11}\ cm^{-2}$ to -1.5 at $n_g \approx 10^{12}\ cm^{-2}$. It is interesting that the exponent measured at lower densities is much closer to one (namely, equal to -3.15) coming from the theory of 2D membranes [53] and appears in theoretical simulations of graphene flexural phonons dynamics [54, 55], which take into account only mechanical degrees of freedom. Ergo, it can be seen that appearance of free electrons causes a significant impact on the corrugation of graphene and, thus, electronic degrees of freedom should not be excluded

from the modeling of graphene structural or mechanical properties. Taking into account that the role of the electronic degrees of freedom in graphene structural characteristics is not well-defined (for example, see [56, 20, 57]) we may suppose that the magnitude of the observed effect may relate to the intrinsic defects or ad-atoms, which unavoidably present in a experimentally studied sheets, since the rest experimental details can not provide this effect on measurements as it is discussed earlier in this work.

The reason of the spectral dependence softening at small q-s and the corresponding amplitude decrease at increased charge carriers density is not obvious. At the first sight, the increasing charge carriers generation by the electron beam leads to the intensification of the charge density fluctuations, that, in turn, is expected to raise the amplitude of the out-of-plane undulations through the coupling of the bending and stretching modes. However, the enhanced screening at the higher carrier density reduces the coupling between electronic and mechanical degrees of freedom. This can be explained as the shift of the crossover q-s, at which the interaction with the charge carriers results in the large anomalies in the flexural phonon spectrum [15, 17, 19], towards zero when the dielectric constant increases. Thus, in the measured wavevector range we observe the opposite effect. However, we have to admit that initially reduced screening in the oxidized graphene may account for the magnitude of the observed effect, which, thus, can be overestimated in comparison to more practically relevant cases.

A note can also be taken concerning the behaviour of the spectrum right-hand part corresponding to the short wavelength undulations. There is an agreement between various theoretical approaches that the spectral dependence must be $^{T}/_{\kappa q^4}$ at this range, where T is the crystal temperature and κ is the bending rigidity. This expression comes from harmonic approximation of 2D membrane mechanics with the only difference that the bending rigidity can vary depending on the spectrum amplitude on the whole scale due to the essential non-linearity of graphene mechanics [12, 58, 59]. Our measurements allow us to suppose that we observe an actual increase of the spectrum intensity at this range with increasing charge carrier density. This increase can not be

attributed to the temperature rise resulting from the enhanced heating of the sheet by more intense electron beam used for producing of the higher density. The expected heating should not exceed 1 K at the given current densities due to the high thermal conductivity of the sheet. At the same time, the corrugation variation with temperature is expected to be proportional to T (or $\sqrt{T}$ for wave-vectors below critical q_c, which is of the order of 1 nm^{-1}) and can be noticed at such degree only at much higher temperature changes [24, 28]. Thus, the observed variation of the spectral amplitude at the short-wavelength range, which is opposite to that at smaller q-s, can be considered as a pure evidence of graphene mechanics non-linearity leading to 15% increase of the bending rigidity in our case (from ca. 1.2 eV to 1.4 eV).

Our finding implies some consequences concerning the variation of graphene electronic properties with charge carriers density. Unfortunately, it is hard to decouple the observed effect with the result of the flexural modes suppression under back gate induced strain in suspended graphene. However, it is expected to be, at least partially, responsible for the non-linear and asymmetrical resistivity dependence on the charge carriers density (i.e. electrostatic doping level) [4, 60, 61, 62] which is more pronounced in suspended devices. Nevertheless, it can be concluded that the suppression of the long-wavelength undulations has to contribute to the enhancement of the charge carriers mobility in the case of increasing electron doping, since the practically relevant values of the Fermi vector lie in the spectral range in which we observe the decrease of the corrugation amplitude.

To conclude, we have discovered the variation of the suspended graphene corrugation with the change of the charge carrier density. The variation is more pronounced at the left-hand part of the corrugation spectrum at $q < 1$ nm^{-1}. This result suggests that the found decrease of the corrugation may result into the decrease of the flexural phonons contribution to the graphene resistivity up to 50%. This may explain some details of the electron mobility dependence on the doping level. The observed phenomenon proves that the consideration of graphene as an electronic membrane is essential for correct

modeling of suspended graphene based devices.

DAK thanks Russian Foundation for Basic Research (project no. 16-32-60165) for support of the 2D crystals surface undulations studies. MVB thanks the Ministry of Education and Science of the Russian Federation (project 3.3161.2017/4.6) for support of the electronic structure investigations. The structural characterizations were performed with the use of the equipment owned by the Joint Research Center Material science and characterization in advanced technology (Ioffe Institute, St.-Petersburg, Russia).

[1] A. K. Geim, K. S. Novoselov, The rise of graphene, Nat. Mater. 6 (3) (2007) 183–191. doi:10.1038/nmat1849.
URL http://www.nature.com/doifinder/10.1038/nmat1849

[2] K. Bolotin, K. Sikes, Z. Jiang, M. Klima, G. Fudenberg, J. Hone, P. Kim, H. Stormer, Ultrahigh electron mobility in suspended graphene, Solid State Commun. 146 (9-10) (2008) 351–355. arXiv:0802.2389, doi:10.1016/j.ssc.2008.02.024.
URL http://linkinghub.elsevier.com/retrieve/pii/S0038109808001178

[3] X. Du, I. Skachko, A. Barker, E. Y. Andrei, Approaching ballistic transport in suspended graphene, Nat. Nanotechnol. 3 (8) (2008) 491–495. arXiv:0802.2933, doi:10.1038/nnano.2008.199.
URL http://www.nature.com/doifinder/10.1038/nnano.2008.199

[4] S. V. Morozov, K. S. Novoselov, M. I. Katsnelson, F. Schedin, D. C. Elias, J. A. Jaszczak, A. K. Geim, Giant Intrinsic Carrier Mobilities in Graphene and Its Bilayer, Phys. Rev. Lett. 100 (1) (2008) 016602. arXiv:0710.5304, doi:10.1103/PhysRevLett.100.016602.
URL https://link.aps.org/doi/10.1103/PhysRevLett.100.016602

[5] A. S. Mayorov, D. C. Elias, I. S. Mukhin, S. V. Morozov, L. A. Ponomarenko, K. S. Novoselov, A. K. Geim, R. V. Gorbachev, How Close Can One Approach the Dirac Point in Graphene Experimentally?, Nano Lett.

12 (9) (2012) 4629–4634. arXiv:1206.3848, doi:10.1021/nl301922d.
URL http://pubs.acs.org/doi/abs/10.1021/nl301922d

[6] M. Katsnelson, A. Geim, Electron scattering on microscopic corrugations in graphene, Philos. Trans. R. Soc. A Math. Phys. Eng. Sci. 366 (1863) (2008) 195–204. arXiv:0706.2490, doi:10.1098/rsta.2007.2157.
URL http://rsta.royalsocietypublishing.org/cgi/doi/10.1098/rsta.2007.2157

[7] N. Abedpour, M. Neek-Amal, R. Asgari, F. Shahbazi, N. Nafari, M. R. R. Tabar, Roughness of undoped graphene and its short-range induced gauge field, Phys. Rev. B 76 (19) (2007) 195407. arXiv:0705.0103, doi:10.1103/PhysRevB.76.195407.
URL https://link.aps.org/doi/10.1103/PhysRevB.76.195407

[8] E. Mariani, F. von Oppen, Flexural Phonons in Free-Standing Graphene, Phys. Rev. Lett. 100 (7) (2008) 076801. arXiv:0707.4350, doi:10.1103/PhysRevLett.100.076801.
URL https://link.aps.org/doi/10.1103/PhysRevLett.100.076801

[9] E. V. Castro, H. Ochoa, M. I. Katsnelson, R. V. Gorbachev, D. C. Elias, K. S. Novoselov, A. K. Geim, F. Guinea, Limits on Charge Carrier Mobility in Suspended Graphene due to Flexural Phonons, Phys. Rev. Lett. 105 (26) (2010) 266601. arXiv:1008.2522, doi:10.1103/PhysRevLett.105.266601.
URL https://link.aps.org/doi/10.1103/PhysRevLett.105.266601

[10] S. Das Sarma, S. Adam, E. H. Hwang, E. Rossi, Electronic transport in two-dimensional graphene, Rev. Mod. Phys. 83 (2) (2011) 407–470. arXiv:1003.4731, doi:10.1103/RevModPhys.83.407.
URL https://link.aps.org/doi/10.1103/RevModPhys.83.407

[11] I. V. Gornyi, V. Y. Kachorovskii, A. D. Mirlin, Conductivity of suspended graphene at the Dirac point, Phys. Rev. B 86 (16) (2012) 165413. doi:

10.1103/PhysRevB.86.165413.
URL https://link.aps.org/doi/10.1103/PhysRevB.86.165413

[12] A. Fasolino, J. H. Los, M. I. Katsnelson, Intrinsic ripples in graphene, Nat. Mater. 6 (11) (2007) 858–861. doi:10.1038/nmat2011.
URL http://arxiv.org/abs/0704.1793{%}0Ahttp://dx.doi.org/10.1038/nmat2011http://www.nature.com/doifinder/10.1038/nmat2011

[13] J. C. Meyer, A. K. Geim, M. I. Katsnelson, K. S. Novoselov, T. J. Booth, S. Roth, The structure of suspended graphene sheets, Nature 446 (7131) (2007) 60–63. doi:10.1038/nature05545.
URL http://www.nature.com/doifinder/10.1038/nature05545

[14] J. Meyer, A. Geim, M. Katsnelson, K. Novoselov, D. Obergfell, S. Roth, C. Girit, A. Zettl, On the roughness of single- and bi-layer graphene membranes, Solid State Commun. 143 (1-2) (2007) 101–109. doi:10.1016/j.ssc.2007.02.047.
URL http://linkinghub.elsevier.com/retrieve/pii/S003810980700316X

[15] J. González, E. Perfetto, Many-body effects on out-of-plane phonons in graphene, New J. Phys. 11 (9) (2009) 095015. doi:10.1088/1367-2630/11/9/095015.
URL http://stacks.iop.org/1367-2630/11/i=9/a=095015?key=crossref.ad5efb096a6ef17df5555dc62145ca3b

[16] M. Gibertini, A. Tomadin, F. Guinea, M. I. Katsnelson, M. Polini, Electron-hole puddles in the absence of charged impurities, Phys. Rev. B 85 (20) (2012) 201405. doi:10.1103/PhysRevB.85.201405.
URL https://link.aps.org/doi/10.1103/PhysRevB.85.201405

[17] D. Gazit, Correlation between charge inhomogeneities and structure in graphene and other electronic crystalline membranes, Phys. Rev. B 80 (16) (2009) 161406. doi:10.1103/PhysRevB.80.161406.
URL https://link.aps.org/doi/10.1103/PhysRevB.80.161406

[18] D. Gazit, Theory of the spontaneous buckling of doped graphene, Phys. Rev. B 79 (11) (2009) 113411. doi:10.1103/PhysRevB.79.113411.
URL https://link.aps.org/doi/10.1103/PhysRevB.79.113411

[19] P. San-Jose, J. González, F. Guinea, Electron-Induced Rippling in Graphene, Phys. Rev. Lett. 106 (4) (2011) 045502. doi:10.1103/PhysRevLett.106.045502.
URL https://link.aps.org/doi/10.1103/PhysRevLett.106.045502

[20] J. González, Rippling transition from electron-induced condensation of curvature field in graphene, Phys. Rev. B 90 (16) (2014) 165402. doi:10.1103/PhysRevB.90.165402.
URL https://link.aps.org/doi/10.1103/PhysRevB.90.165402

[21] F. Guinea, P. Le Doussal, K. J. Wiese, Collective excitations in a large-<math> <mi>d</mi> </math> model for graphene, Phys. Rev. B 89 (12) (2014) 125428. doi:10.1103/PhysRevB.89.125428.
URL https://link.aps.org/doi/10.1103/PhysRevB.89.125428

[22] H. Ochoa, E. V. Castro, M. Katsnelson, F. Guinea, Scattering by flexural phonons in suspended graphene under back gate induced strain, Phys. E Low-dimensional Syst. Nanostructures 44 (6) (2012) 963–966. doi:10.1016/j.physe.2011.03.017.
URL http://linkinghub.elsevier.com/retrieve/pii/S1386947711000919

[23] N. R. Wilson, P. A. Pandey, R. Beanland, J. P. Rourke, U. Lupo, G. Rowlands, R. A. Römer, On the structure and topography of free-standing chemically modified graphene, New J. Phys. 12 (12) (2010) 125010. doi:10.1088/1367-2630/12/12/125010.
URL http://stacks.iop.org/1367-2630/12/i=12/a=125010?key=crossref.49c84637606c4de33e8c20b4a4e05463

[24] A. Locatelli, K. R. Knox, D. Cvetko, T. O. Mentes, M. A. Nino, S. Wang,

M. B. Yilmaz, P. Kim, R. M. Osgood, A. Morgante, Corrugation in Exfoliated Graphene: An Electron Microscopy and Diffraction Study, ACS Nano 4 (8) (2010) 4879–4889. doi:10.1021/nn101116n.
URL http://pubs.acs.org/doi/abs/10.1021/nn101116n

[25] D. A. Kirilenko, A. T. Dideykin, G. Van Tendeloo, Measuring the corrugation amplitude of suspended and supported graphene, Phys. Rev. B - Condens. Matter Mater. Phys. 84 (23) (2011) 1–5. doi:10.1103/PhysRevB.84.235417.

[26] B. Shevitski, M. Mecklenburg, W. A. Hubbard, E. R. White, B. Dawson, M. S. Lodge, M. Ishigami, B. C. Regan, Dark-field transmission electron microscopy and the Debye-Waller factor of graphene, Phys. Rev. B 87 (4) (2013) 045417. doi:10.1103/PhysRevB.87.045417.
URL https://link.aps.org/doi/10.1103/PhysRevB.87.045417

[27] D. A. Kirilenko, Electron diffraction measurement of the binding rigidity of free-standing graphene, Tech. Phys. Lett. 39 (4) (2013) 325–328. doi:Doi10.1134/S1063785013040081.

[28] C. S. Allen, E. Liberti, J. S. Kim, Q. Xu, Y. Fan, K. He, A. W. Robertson, H. W. Zandbergen, J. H. Warner, A. I. Kirkland, Temperature dependence of atomic vibrations in mono-layer graphene, J. Appl. Phys. 118 (7) (2015) 074302. doi:10.1063/1.4928324.
URL http://aip.scitation.org/doi/10.1063/1.4928324

[29] A. Dideykin, A. Aleksenskiy, D. Kirilenko, P. Brunkov, V. Goncharov, M. Baidakova, D. Sakseev, A. Ya.Vul', Monolayer graphene from graphite oxide, Diam. Relat. Mater. 20 (2) (2011) 105–108. doi:10.1016/j.diamond.2010.10.007.
URL http://linkinghub.elsevier.com/retrieve/pii/S092596351000302X

[30] V. M. Mikoushkin, V. V. Shnitov, S. Y. Nikonov, A. T. Dideykin, S. P. Vul', A. Y. Vul', D. A. Sakseev, D. V. Vyalikh, O. Y. Vilkov, Controlling

graphite oxide bandgap width by reduction in hydrogen, Tech. Phys. Lett. 37 (10) (2011) 942–945. doi:10.1134/S1063785011100257.
URL http://link.springer.com/10.1134/S1063785011100257

[31] A. Mathkar, D. Tozier, P. Cox, P. Ong, C. Galande, K. Balakrishnan, A. Leela Mohana Reddy, P. M. Ajayan, Controlled, Stepwise Reduction and Band Gap Manipulation of Graphene Oxide, J. Phys. Chem. Lett. 3 (8) (2012) 986–991. doi:10.1021/jz300096t.
URL http://pubs.acs.org/doi/abs/10.1021/jz300096t

[32] M. Acik, Y. J. Chabal, A Review on Reducing Graphene Oxide for Band Gap Engineering, J. Mater. Sci. Res. 2 (1) (2012) 101–112. doi:10.5539/jmsr.v2n1p101.
URL http://www.ccsenet.org/journal/index.php/jmsr/article/view/20352

[33] X.-F. Zhang, X. Shao, S. Liu, Dual Fluorescence of Graphene Oxide: A Time-Resolved Study, J. Phys. Chem. A 116 (27) (2012) 7308–7313. doi:10.1021/jp301755b.
URL http://pubs.acs.org/doi/abs/10.1021/jp301755b

[34] D. Du, H. Song, Y. Nie, X. Sun, L. Chen, J. Ouyang, Photoluminescence of Graphene Oxide in Visible Range Arising from Excimer Formation, J. Phys. Chem. C 119 (34) (2015) 20085–20090. doi:10.1021/acs.jpcc.5b04529.
URL http://pubs.acs.org/doi/10.1021/acs.jpcc.5b04529

[35] J. M. Dawlaty, S. Shivaraman, M. Chandrashekhar, F. Rana, M. G. Spencer, Measurement of ultrafast carrier dynamics in epitaxial graphene, Appl. Phys. Lett. 92 (4) (2008) 042116. doi:10.1063/1.2837539.
URL http://aip.scitation.org/doi/10.1063/1.2837539

[36] M. Breusing, C. Ropers, T. Elsaesser, Ultrafast Carrier Dynamics in Graphite, Phys. Rev. Lett. 102 (8) (2009) 086809. doi:10.1103/PhysRevLett.102.086809.
URL https://link.aps.org/doi/10.1103/PhysRevLett.102.086809

[37] S. K. Singh, S. G. Srinivasan, M. Neek-Amal, S. Costamagna, A. C. T. van Duin, F. M. Peeters, Thermal properties of fluorinated graphene, Phys. Rev. B 87 (10) (2013) 104114. doi:10.1103/PhysRevB.87.104114.
URL https://link.aps.org/doi/10.1103/PhysRevB.87.104114

[38] J. W. Wilson, Y. J. Xu, E. Kamaratos, C. Chang, Mean Excitation Energies for Stopping Powers in Various Materials Using Local Plasma Oscillator Strengths, NASA Tech. Pap. 2271.
URL https://ntrs.nasa.gov/archive/nasa/casi.ntrs.nasa.gov/19840013417.pdf

[39] J. C. Meyer, F. Eder, S. Kurasch, V. Skakalova, J. Kotakoski, H. J. Park, S. Roth, A. Chuvilin, S. Eyhusen, G. Benner, A. V. Krasheninnikov, U. Kaiser, Accurate Measurement of Electron Beam Induced Displacement Cross Sections for Single-Layer Graphene, Phys. Rev. Lett. 108 (19) (2012) 196102. doi:10.1103/PhysRevLett.108.196102.
URL https://link.aps.org/doi/10.1103/PhysRevLett.108.196102

[40] A. A. Balandin, S. Ghosh, W. Bao, I. Calizo, D. Teweldebrhan, F. Miao, C. N. Lau, Superior Thermal Conductivity of Single-Layer Graphene, Nano Lett. 8 (3) (2008) 902–907. doi:10.1021/nl0731872.
URL http://pubs.acs.org/doi/abs/10.1021/nl0731872

[41] S. Ghosh, I. Calizo, D. Teweldebrhan, E. P. Pokatilov, D. L. Nika, A. A. Balandin, W. Bao, F. Miao, C. N. Lau, Extremely high thermal conductivity of graphene: Prospects for thermal management applications in nanoelectronic circuits, Appl. Phys. Lett. 92 (15) (2008) 151911. doi:10.1063/1.2907977.
URL http://aip.scitation.org/doi/10.1063/1.2907977

[42] J.-U. Lee, D. Yoon, H. Kim, S. W. Lee, H. Cheong, Thermal conductivity of suspended pristine graphene measured by Raman spectroscopy, Phys. Rev. B 83 (8) (2011) 081419. doi:10.1103/PhysRevB.83.081419.
URL https://link.aps.org/doi/10.1103/PhysRevB.83.081419

[43] J.-H. Zou, B.-Y. Cao, Phonon thermal properties of graphene on h -BN from molecular dynamics simulations, Appl. Phys. Lett. 110 (10) (2017) 103106. doi:10.1063/1.4978434.
URL http://aip.scitation.org/doi/10.1063/1.4978434

[44] Z. Ni, Q. Liu, K. Tang, J. Zheng, J. Zhou, R. Qin, Z. Gao, D. Yu, J. Lu, Tunable Bandgap in Silicene and Germanene, Nano Lett. 12 (1) (2012) 113–118. doi:10.1021/nl203065e.
URL http://pubs.acs.org/doi/abs/10.1021/nl203065e

[45] M. D. Kamatagi, A. S. Nissimagoudar, N. S. Sankeshwar, B. G. Mulimani, Lattice thermal conductivity of graphene, Vol. 946, 2012, pp. 945–946. doi:10.1063/1.4710315.
URL http://aip.scitation.org/doi/abs/10.1063/1.4710315

[46] K. V. Zakharchenko, M. I. Katsnelson, A. Fasolino, Finite temperature lattice properties of graphene beyond the quasiharmonic approximation, Phys. Rev. Lett. 102 (4) (2009) 2–5. arXiv:0812.4184, doi:10.1103/PhysRevLett.102.046808.

[47] A. L. C. da Silva, L. Cândido, J. N. Teixeira Rabelo, G.-Q. Hai, F. M. Peeters, Anharmonic effects on thermodynamic properties of a graphene monolayer, EPL (Europhysics Lett. 107 (5) (2014) 56004. doi:10.1209/0295-5075/107/56004.
URL http://stacks.iop.org/0295-5075/107/i=5/a=56004?key=crossref.686d4e3159cdb115845f27ce4779b57d

[48] K. H. Michel, S. Costamagna, F. M. Peeters, Theory of thermal expansion in 2D crystals, Phys. status solidi 252 (11) (2015) 2433–2437. doi:10.1002/pssb.201552286.
URL http://doi.wiley.com/10.1002/pssb.201552286

[49] I. S. Burmistrov, I. V. Gornyi, V. Y. Kachorovskii, M. I. Katsnelson, A. D. Mirlin, Quantum elasticity of graphene: Thermal expansion coefficient and

specific heat, Phys. Rev. B 94 (19) (2016) 195430. arXiv:1609.00924, doi:10.1103/PhysRevB.94.195430.
URL https://link.aps.org/doi/10.1103/PhysRevB.94.195430

[50] R. Roldán, A. Fasolino, K. V. Zakharchenko, M. I. Katsnelson, Suppression of anharmonicities in crystalline membranes by external strain, Phys. Rev. B 83 (17) (2011) 174104. arXiv:1101.6026, doi:10.1103/PhysRevB.83.174104.
URL https://link.aps.org/doi/10.1103/PhysRevB.83.174104

[51] B. Amorim, A. Cortijo, F. de Juan, A. Grushin, F. Guinea, A. Gutiérrez-Rubio, H. Ochoa, V. Parente, R. Roldán, P. San-Jose, J. Schiefele, M. Sturla, M. Vozmediano, Novel effects of strains in graphene and other two dimensional materials, Phys. Rep. 617 (2016) 1–54. arXiv:1503.00747, doi:10.1016/j.physrep.2015.12.006.
URL http://dx.doi.org/10.1016/j.physrep.2015.12.006http://linkinghub.elsevier.com/retrieve/pii/S0370157315005402

[52] D. A. Kirilenko, P. N. Brunkov, Measuring the height-to-height correlation function of corrugation in suspended graphene, Ultramicroscopy 165 (2016) 1–7. doi:10.1016/j.ultramic.2016.03.010.
URL http://dx.doi.org/10.1016/j.ultramic.2016.03.010

[53] D. Nelson, L. Peliti, Fluctuations in membranes with crystalline and hexatic order, J. Phys. 48 (7) (1987) 1085–1092. doi:10.1051/jphys:019870048070108500.
URL http://www.edpsciences.org/10.1051/jphys:019870048070108500

[54] J. H. Los, M. I. Katsnelson, O. V. Yazyev, K. V. Zakharchenko, A. Fasolino, Scaling properties of flexible membranes from atomistic simulations: Application to graphene, Phys. Rev. B 80 (12) (2009) 121405. doi:10.1103/PhysRevB.80.121405.
URL https://link.aps.org/doi/10.1103/PhysRevB.80.121405

[55] K. V. Zakharchenko, R. Roldán, A. Fasolino, M. I. Katsnelson, Self-consistent screening approximation for flexible membranes: Application to graphene, Phys. Rev. B 82 (12) (2010) 125435. doi:10.1103/PhysRevB.82.125435.
URL https://link.aps.org/doi/10.1103/PhysRevB.82.125435

[56] P. Partovi-Azar, N. Nafari, M. R. R. Tabar, Interplay between geometrical structure and electronic properties in rippled free-standing graphene, Phys. Rev. B 83 (16) (2011) 165434. doi:10.1103/PhysRevB.83.165434.
URL https://link.aps.org/doi/10.1103/PhysRevB.83.165434

[57] B. Amorim, R. Roldán, E. Cappelluti, A. Fasolino, F. Guinea, M. I. Katsnelson, Thermodynamics of quantum crystalline membranes, Phys. Rev. B 89 (22) (2014) 224307. arXiv:1403.2637, doi:10.1103/PhysRevB.89.224307.
URL https://link.aps.org/doi/10.1103/PhysRevB.90.176301https://link.aps.org/doi/10.1103/PhysRevB.89.224307

[58] F. L. Braghin, N. Hasselmann, Thermal fluctuations of free-standing graphene, Phys. Rev. B 82 (3) (2010) 035407. doi:10.1103/PhysRevB.82.035407.
URL https://link.aps.org/doi/10.1103/PhysRevB.82.035407

[59] R. Ramírez, E. Chacón, C. P. Herrero, Anharmonic effects in the optical and acoustic bending modes of graphene, Phys. Rev. B 93 (23) (2016) 235419. doi:10.1103/PhysRevB.93.235419.
URL https://link.aps.org/doi/10.1103/PhysRevB.93.235419

[60] K. I. Bolotin, K. J. Sikes, J. Hone, H. L. Stormer, P. Kim, Temperature-Dependent Transport in Suspended Graphene, Phys. Rev. Lett. 101 (9) (2008) 096802. doi:10.1103/PhysRevLett.101.096802.
URL https://link.aps.org/doi/10.1103/PhysRevLett.101.096802

[61] J.-H. Chen, C. Jang, S. Xiao, M. Ishigami, M. S. Fuhrer, Intrinsic and extrinsic performance limits of graphene devices on SiO2, Nat. Nanotechnol.

3 (4) (2008) 206–209. doi:10.1038/nnano.2008.58.
URL http://www.nature.com/doifinder/10.1038/nnano.2008.58

[62] D. K. Efetov, P. Kim, Controlling Electron-Phonon Interactions in Graphene at Ultrahigh Carrier Densities, Phys. Rev. Lett. 105 (25) (2010) 256805. doi:10.1103/PhysRevLett.105.256805.
URL https://link.aps.org/doi/10.1103/PhysRevLett.105.256805

- Strain-free charge carriers generation technique is used.
- Strong influence of charge carriers on the corrugation of graphene is observed.
- So, this mechanism can not be omitted at a proper modeling of graphene properties.